

Syntheses, Crystal Structures, Visible, and Near-Infrared Luminescence Properties of 3d–4f Coordination Polymers Cu_2Er_2 and Eu_2Ni_2

L. X. Zhong^a, M. Y. Liu^a, B. W. Zhang^a, Y. Q. Sun^{a, b, *}, Y. Y. Xu^{a, *}, and D. Z. Gao^a

^aTianjin Key Laboratory of Structure and Performance for Functional Molecule, College of Chemistry, Tianjin Normal University, Tianjin, 300387 P.R. China

^bKey Laboratory of Advanced Energy Materials Chemistry (Ministry of Education), Nankai University, Tianjin, 300071 P.R. China

*e-mail: hxxysyq@mail.tjnu.edu.cn

Received December 1, 2018; revised June 18, 2019; accepted June 27, 2019

Abstract—Solvothermal condition reaction of $\text{Ln}(\text{NO}_3)_3 \cdot 6\text{H}_2\text{O}$ ($\text{Ln} = \text{Er, Eu}$) with 5-nitroisophthalate (Nipt^{2-}) and mononuclear macrocyclic oxamide complex ML ($\text{M} = \text{Ni or Cu}$) afforded two new 3d–4f heterometallic coordination polymers $[\text{Er}_2(\text{CuL})_2(\text{Nipt})_3(\text{H}_2\text{O})] \cdot 0.75\text{H}_2\text{O}$ (**I**) and $[\text{Eu}_2(\text{NiL})_2(\text{Nipt})_3(\text{H}_2\text{O})] \cdot \text{H}_2\text{O}$ (**II**) (ML , $\text{H}_2\text{L} = 2,3\text{-dioxo-5,6,14,15-dibenzo-1,4,8,12-tetraazacyclo-pentadeca-7,13-dien}$; $\text{H}_2\text{Nipt} = 5\text{-nitroisophthalic acid}$). Their structures have been characterized by elemental analyses, FT-IR, UV, and single-crystal X-ray diffraction analyses (CIF files CCDC nos. 1880429 (**I**), 1880430 (**II**)). Both complexes **I** and **II** exhibit a 2D dimensional heterometallic framework with 3,3,4,5-connected $(3^2.4^2.5.6^3.7^2)(4^2.6^3.8)(4^2.6)$ topology, and adjacent 2D structures are connect together with intermolecular $\text{O}-\text{H}\cdots\text{O}$ and $\text{C}-\text{H}\cdots\text{O}$ hydrogen bonds to form a 3D supermolecular architectures. Moreover, the visible and near-infrared luminescence properties of the compound **I** are also discussed.

Keywords: 3d–4f coordination polymers, macrocyclic oxamide complex, luminescence properties, single-crystal X-ray diffraction analysis

DOI: 10.1134/S1070328420040090

INTRODUCTION

The search for new compound with exciting magnetic, luminescent and other functional characteristics promoted chemists to combine two or more different metal ions within the same molecule or framework [1–5]. Especially, the 3d–4f heterometallic coordination polymers (CPs) have captivated more and more researchers due to their potential applications in various scientific fields, for example, magnet, gas adsorption/separation, catalyst, luminescence, etc. [1, 6–11]. Up to now, although a large number of 3d–4f CPs with different morphologies, structure and dimensions have been reported [12–17], it has still been a challenge to predict the final architectures of 3d–4f CPs. Therefore, it is necessary to choose a simple and high-efficiency experiment method. In recent years, utilizing ‘metalloligand’ synthetic approach to construct 3d–4f coordination frameworks has attracted a great deal of attentions, because this method is easy controllable and beneficial to design and modulate the structures [1, 18]. Compared with other metalloligands, mononuclear macrocyclic oxamide ligands are stable, easy to control in the synthesis process, and not easy to produce other impurities, but their

biggest drawback is that the coordination polymers with one-, two- or three-dimensionality are hard to obtain. Thus, in this paper, we adopt a mixed-ligand self-assembly synthetic method, that is, using carboxylate organic ligand and mononuclear macrocyclic oxamide ML (Scheme 1a) as co-ligands to construct novel 3d–4f CPs. Because carboxylate organic ligand and its ions have been proven to be good linkers [19–21], due to their versatile coordination modes, strong coordination ability with Ln^{3+} ions. Moreover, the degree of protonation of carboxylate organic ligands affects the number of the functional coordination sites, and provides endless possible outcomes of the final products. With these facts in mind and in continuation of our interest in X-ray diffraction analyses CPs, in this work, we use 5-nitroisophthalate and mononuclear macrocyclic oxamide ML as mixed ligands to react with Ln^{3+} ions. The results show that two novel coordination polymers $[\text{Er}_2(\text{CuL})_2(\text{Nipt})_3(\text{H}_2\text{O})] \cdot 0.75\text{H}_2\text{O}$ (**I**) and $[\text{Eu}_2(\text{NiL})_2(\text{Nipt})_3(\text{H}_2\text{O})] \cdot \text{H}_2\text{O}$ (**II**) were obtained. More interestingly, the nitro group (NO_2) as an electron-withdrawing coexisting in isophthalic can weakly coordinate with transition metal ions M(II) ($\text{M} = \text{Cu, Ni}$) in

CPs **I** and **II**, to the best of our knowledge, which is very rare. Considering the synergistic effect between lanthanide and transition metal ions and the different ligands, we investigate the luminescence of complex **I**. The results show that mononuclear macrocyclic oxamide CuL can serve as an efficient sensitizer for the near-infrared luminescence of trivalent erbium ion. Although the researches about the near-infrared (NIR) emission of lanthanide complexes containing Yb(III), Nd(III) and Er(III) have become a hot topic due to the potential applications in bioassays and laser system [22–28], the light-absorbing Cu(II)L chromophores used as sensitizers for NIR luminescence has not been reported.

EXPERIMENTAL

All the starting reagents were purchased and used without further purification. The complex ligand ML ($M = \text{Cu, Ni}$) was prepared according to the described elsewhere [29]. Elemental analyses for C, H and N were carried out with a Perkin-Elmer 240 Elemental analyzer. IR spectra ($600\text{--}4000\text{ cm}^{-1}$) were measured with a KBr plate on a Shimadzu IR-408 infrared spectrophotometer. Electronic spectra for solid samples were recorded on a Shimadzu UV-2101 PC scanning spectrophotometer. The luminescence properties were carried out on a RF-5301PC luminescence.

Synthesis of complex I. A mixture of $\text{Er}(\text{NO}_3)_3 \cdot 6\text{H}_2\text{O}$ (0.05 mmol, 23.1 mg), CuL (0.1 mmol, 19.6 mg), H_2Nipt (0.1 mmol, 21 mg), H_2O (10 mL) and CH_3OH (4 mL) was placed in a 25 mL-Teflon-lined reactor and stirred for 30 min at room temperature, and then triethylamine was dropped in until the pH value of the system was adjusted to about 7–8. The reaction mixture was sealed and heated at 160°C for 72 h and then cooled to room temperature. Dark green crystals of complex **I** suitable for single crystal X-ray diffraction analysis had been produced and washed several times by distilled water. The yield was 40.1%.

For $\text{C}_{62}\text{H}_{44.5}\text{N}_{11}\text{O}_{24}\text{Cu}_2\text{Er}_2$ (**I**)

Anal. calcd., %	C, 41.58	H, 2.49	N, 8.61
Found, %	C, 41.60	H, 2.52	N, 8.65

IR bands ($\nu, \text{ cm}^{-1}$): 1635 $\nu(\text{COO}^-)$, 1611 $\nu(\text{C=O})$, 1541 $\nu(\text{C=N})$, 1338 $\nu(\text{NO}_2)$.

Synthesis of complex II was carried out by the same way as **I**, but using $\text{Eu}(\text{NO}_3)_3 \cdot 6\text{H}_2\text{O}$ (0.05 mmol, 22.3 mg) instead of $\text{Er}(\text{NO}_3)_3 \cdot 6\text{H}_2\text{O}$, and using NiL (0.05 mmol) instead of CuL. Finally, the red crystals were obtained. The yield was 51.3%.

For $\text{C}_{62}\text{H}_{45}\text{N}_{11}\text{O}_{24}\text{Ni}_2\text{Eu}_2$ (**II**)

Anal. calcd., %	C, 42.54	H, 2.57	N, 8.80
Found, %	C, 42.57	H, 2.52	N, 8.83

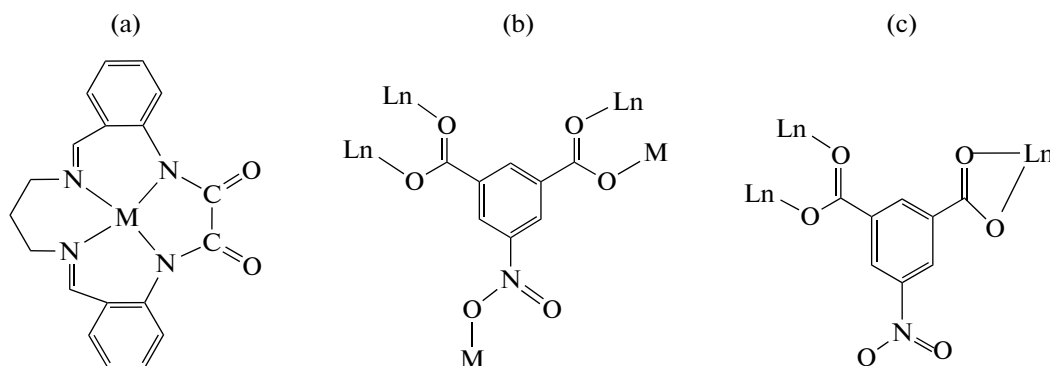
IR bands ($\nu, \text{ cm}^{-1}$): 1643 $\nu(\text{COO}^-)$, 1607 $\nu(\text{C=O})$, 1557 $\nu(\text{C=N})$, 1349 $\nu(\text{NO}_2)$.

X-ray crystallography. All the data for **I**, **II** were collected with a Bruker Smart CCD area detector by using graphite monochromatic MoK_α radiation ($\lambda = 0.71073\text{ \AA}$) at 296.15 K . Using Olex2, the structure was solved with the XS structure solution program using Direct Methods and refined with the ShelXL refinement package using Least Squares minimisation. Hydrogen atoms were added geometrically and refined with riding model position parameters and fixed isotropic thermal parameters. The crystallographic data for **I** and **II** are listed in Table 1, and selected bond lengths and angles for **I** and **II** are summarized in Table 2.

Supplementary material for structures **I** has been deposited with the Cambridge Crystallographic Data Centre (CCDC nos. 1880429 (**I**), 1880430 (**II**); deposit@ccdc.cam.ac.uk or <http://www.ccdc.cam.ac.uk>).

RESULTS AND DISCUSSION

The macrocyclic oxamide complex ligands ML ($M = \text{Cu(II), Ni(II)}$ (a); the coordinated modes of 5-nitroisophthalate ($M = \text{Cu(II), Ni(II)}$); $\text{Ln} = \text{Er(III), Eu(III)}$ (b, c) are given in Scheme 1.



Scheme 1.

Table 1. Crystal data and structure refinement for complexes **I** and **II**

Parameter	Value	
	I	II
Formula weight	1789.19	1749.43
Crystal system	Triclinic	Triclinic
Space group	<i>P</i> 1̄	<i>P</i> 1̄
<i>a</i> , Å	10.701(2)	10.7649(15)
<i>b</i> , Å	14.861(3)	14.8593(19)
<i>c</i> , Å	21.354(5)	21.431(3)
α , deg	95.110(3)	94.388(3)
β , deg	103.256(3)	103.572(3)
γ , deg	109.730(3)	109.847(3)
<i>V</i> , Å ³	3059.5(11)	3088.4(7)
<i>Z</i>	2	2
ρ_{calced} , mg/m ³	1.942	1.881
Absorption coefficient, mm ⁻¹	3.497	2.699
<i>F</i> (000)	1759.0	1736.0
Crystal size, mm	0.18 × 0.15 × 0.14	0.18 × 0.17 × 0.15
Goodness-of-fit on <i>F</i> ²	1.014	0.996
<i>R</i> ₁ (<i>I</i> > 2 σ (<i>I</i>))*	0.0360	0.0770
<i>wR</i> ₂ (all data)*	0.0870	0.2000
Largest diff. peak and hole, e Å ⁻³	1.85/-1.23	3.33/-2.62

* $R_1 = \sum |F_{\text{o}}| - |F_{\text{c}}| / \sum |F_{\text{o}}|$, $wR_2 = \{\sum [w(F_{\text{o}}^2 - F_{\text{c}}^2)^2] / \sum [w(F_{\text{o}})^2]\}^{1/2}$.

Table 2. The data of selected bond distances (Å) and angles (deg) for complexes **I** and **II***

Bond	<i>d</i> , Å	Angle	ω , deg
I			
Er(2)–O(18)	2.645(4)	O(12)Er(1)O(2)	149.52(15)
Er(1)–O(8) ^{#2}	2.216(4)	O(5)Er(1)O(6)	53.84(15)
Er(1)–O(2)	2.354(4)	O(2)Er(1)O(5)	86.91(16)
Er(1)–O(6)	2.418(4)	O(6)Er(1)O(1)	116.27(14)
Cu(2)–N(6)	2.021(6)	N(7)Cu(2)N(5)	171.1(2)
Cu(1)–N(4)	1.957(5)	N(7)Cu(2)N(8)	83.37(19)
II			
Eu(2)–(19) ^{#4}	2.664(10)	O(12)Eu(1)O(2)	149.8(3)
Eu(1)–O(8) ^{#2}	2.264(9)	O(6)Eu(1)O(5)	53.2(3)
Eu(1)–O(2)	2.424(8)	O(5)Eu(1)O(1)	115.5(3)
Eu(2)–O(3)	2.432(8)	O(2)Eu(1)O(5)	79.6(3)
Ni(2)–N(5)	2.010(11)	N(8)Ni(2)N(6)	171.9(6)
Ni(1)–N(3)	1.933(13)	N(8)Ni(2)N(5)	83.4(4)

* Symmetry codes: ^{#2} 1 + *x*, *y*, *z* (**I**); ^{#2} -1 + *x*, *y*, *z*; ^{#4} 1 + *x*, *y*, *z* (**II**).

As revealed by single-crystal X-ray diffraction analysis, there are crystallographically independent two Er^{3+} ions, two Cu^{2+} ions in complex **I**. As shown in Fig. 1a, the $\text{Er}(1)$ ion has eight coordination sites which are occupied by five oxygen atoms from four Nipt^{2-} ligands, two oxygen atoms from one CuL , and an oxygen atom from the coordination water molecule, to furnish a distorted square anti-prism coordination geometry. The $\text{Er}(1)-\text{O}$ bond lengths and $\text{OEr}(1)\text{O}$ bond angles are in the range of 2.216(4)–2.459(4) Å and 53.84(15)°–156.85(15)°, respectively. The $\text{Er}(2)$ ion also resides in a distorted square anti-prism coordination environment with six carboxyl oxygen atoms from five Nipt^{2-} ligands, two oxygen atoms from one CuL . The $\text{Er}(2)-\text{O}$ bond lengths and $\text{OEr}(2)\text{O}$ bond angles are in the range of 2.231(4)–2.645(4) Å and 51.48(13)°–145.87(14)°, respectively. The coordination geometry of each Cu^{2+} ion is a distorted square pyramid surrounded by four nitrogen atoms from macrocyclic oxamide group ($\text{Cu}(1)-\text{N}$ 1.957(5)–1.975(5) Å and $\text{Cu}(2)-\text{N}$ 1.972(5)–2.021(6) Å) and one oxygen atom from COO^- for $\text{Cu}(2)$, NO_2 for $\text{Cu}(1)$ ($\text{Cu}(1)-\text{O}$ 2.829(6) Å and $\text{Cu}(2)-\text{O}$ 2.462(5) Å). Obviously, the axial $\text{Cu}-\text{O}$ bands are weak, which may be related to the Jahn-Teller effect and/or weak coordination ability of nitro group as an electron-withdrawing coexisting in isophthalic. The centre Er^{3+} ions and external Cu^{2+} ions are bridged by oxamide groups to form heterobinuclear units $\text{Er}(1)\text{Cu}(1)$ ($\text{Er}(1)-\text{Cu}(1)$ 5.716(4) Å) and $\text{Er}(2)\text{Cu}(2)$ ($\text{Er}(2)-\text{Cu}(2)$ 5.670(4) Å). $\text{Er}(1)\text{Cu}(1)$ and $\text{Er}(2)\text{Cu}(2)$ heterobinuclear units are interlinked through a Nipt^{2-} to form a asymmetric heterotetrานuclear Cu_2Er_2 unit. The adjacent asymmetric heterotetrานuclear Cu_2Er_2 units are bridged by Nipt^{2-} ligands to afford a 2D dimensional network (Fig. 2). In 2D framework, one kind of Nipt^{2-} connects three Er^{3+} and two Cu^{2+} ions in the order of CuErErCuEr with two $\mu_2\text{-}\eta^1\text{:}\eta^1$ -carboxylate and $\mu_1\text{-}\eta^1$ -nitrogroups (Scheme 1b); another kind of Nipt^{2-} links three Er^{3+} ions adopting $\mu_1\text{-}\eta^1\text{:}\eta^1$ -chelating and $\mu_2\text{-}\eta^1\text{:}\eta^1$ -bridging coordination modes (Scheme 1c). Topologically, the structure is composed of two kinds of 3-connecting Nipt^{2-} anions, 4-connecting and 5-connecting Er^{3+} ions. Thus compound **I** can be simplified to a 3,3,4,5-connected 4-nodal network with the Schläfli symbols of $(3.4.5)(3^2.4^2.5.6^3.7^2)(4^2.6^3.8)(4^2.6)$ (Fig. 3). Furthermore, the adjacent 2D networks are linked together with $\text{O}-\text{H}\cdots\text{O}$ and $\text{C}-\text{H}\cdots\text{O}$ intermolecular hydrogen bonds to form a 3D framework, and $\text{O}\cdots\text{O}$, $\text{C}\cdots\text{O}$ distances and $\text{O}-\text{H}\cdots\text{O}$, $\text{C}-\text{H}\cdots\text{O}$ angles are in the range of 2.765–2.936 Å, 2.804–3.444 Å, 1240°–174° and 119°–164°, respectively.

Single-crystal X-ray diffraction analysis indicated that the compound **II** has the same structure as compound **I**. As shown in Fig. 1b, $\text{Eu}(1)$ ion is eight-coordinated with five O atoms from four the Nipt^{2-}

ligands, two O atoms from one NiL , and one O atom from the coordinated water molecule, the $\text{Eu}(1)-\text{O}$ bond lengths and $\text{OEu}(1)\text{O}$ bond angles are in the range of 2.264(9)–2.514(8) Å and 53.2(3)°–157.4(3)°, respectively. While $\text{Eu}(2)$ ion is also eight-coordinated with six O atoms from five Nipt^{2-} ligands, two O atoms from one NiL , the $\text{Eu}(2)-\text{O}$ bond lengths and $\text{OEu}(2)\text{O}$ bond angles are in the range of 2.291(9)–2.664(1) Å and 50.8(3)°–146.2(3)°, respectively. Each Ni^{2+} ion resides in a distorted square pyramid surrounded by four nitrogen atoms from macrocyclic oxamide group ($\text{Ni}(1)-\text{N}$ 1.933(13)–1.969(10) Å and $\text{Ni}(2)-\text{N}$ 1.962(10)–2.010(11) Å) and one oxygen atom from COO^- for $\text{Ni}(2)$, NO_2 for $\text{Ni}(1)$ ($\text{Ni}(1)-\text{O}$ 2.820(3) Å and $\text{Ni}(2)-\text{O}$ 2.443(6) Å), obviously, the axial $\text{Ni}-\text{O}$ bands are weak. Each Eu^{3+} ion connects one Ni^{2+} ion by oxamide group to form heterobinuclear units $\text{Eu}(1)\text{Ni}(1)$ ($\text{Er}(1)-\text{Ni}(1)$ 5.767(2) Å) and $\text{Eu}(2)\text{Ni}(2)$ ($\text{Er}(2)-\text{Ni}(2)$ 5.710(8) Å), and the two heterobinuclear units are interlinked through a Nipt^{2-} to form a asymmetric heterotetrานuclear Eu_2Ni_2 unit. The adjacent asymmetric heterotetrานuclear Cu_2Eu_2 units are bridged by Nipt^{2-} ligands to afford a 2D dimensional network, which is similar to that of complex **I** (Fig. 2). Furthermore, the adjacent 2D networks are bridged together with $\text{O}-\text{H}\cdots\text{O}$ and $\text{C}-\text{H}\cdots\text{O}$ intermolecular hydrogen bonds to form a 3D framework, and $\text{O}\cdots\text{O}$, $\text{C}\cdots\text{O}$ distances and $\text{O}-\text{H}\cdots\text{O}$, $\text{C}-\text{H}\cdots\text{O}$ angles are in the range of 2.753–3.021 Å, 2.805–3.465 Å, 119°–135° and 120°–152°, respectively.

For complexes **I** and **II**, the strong peaks in the range 1635–1643 and 1389–1366 cm^{-1} are characteristic of the absorption for the asymmetric and symmetric stretching vibrations of COO^- , and all carboxyl groups of H_2Nipt are deprotonated because no bands for COOH in the region 1680–1720 cm^{-1} were observed [30]. The bands around 1338–1349 cm^{-1} are characteristic of the nitro group [30]. The characteristic absorption peaks of mononuclear macrocyclic oxamide ligands ML appear in range of 1601–1617 and 1547–1560 cm^{-1} , which are attributed to the $\nu(\text{C}=\text{O})$ and the $\nu(\text{C}=\text{N})$ vibrations [30], respectively. The bands around 3421 cm^{-1} are characteristic of the hydroxyl from H_2O [30].

The solid-state electronic absorption spectra were measured at room temperature. For **I** and **II**, the broad absorption band at 634 and 580 nm can be designed to the spin-allowed $d-d$ electronic transition of Cu^{2+} and Ni^{2+} ions in C_{4v} [31], respectively, compared with ML , **I** and **II** both have a red shift. Below 500 nm, the complexes exhibit intense bands, which are related to the charge-transfer transitions in the $[\text{ML}]$ ($\text{M} = \text{Cu, Ni}$) chromophores and/or intraligand $\pi-\pi^*$ transitions [31]. The hypersensitive transition bands of the Er^{3+}

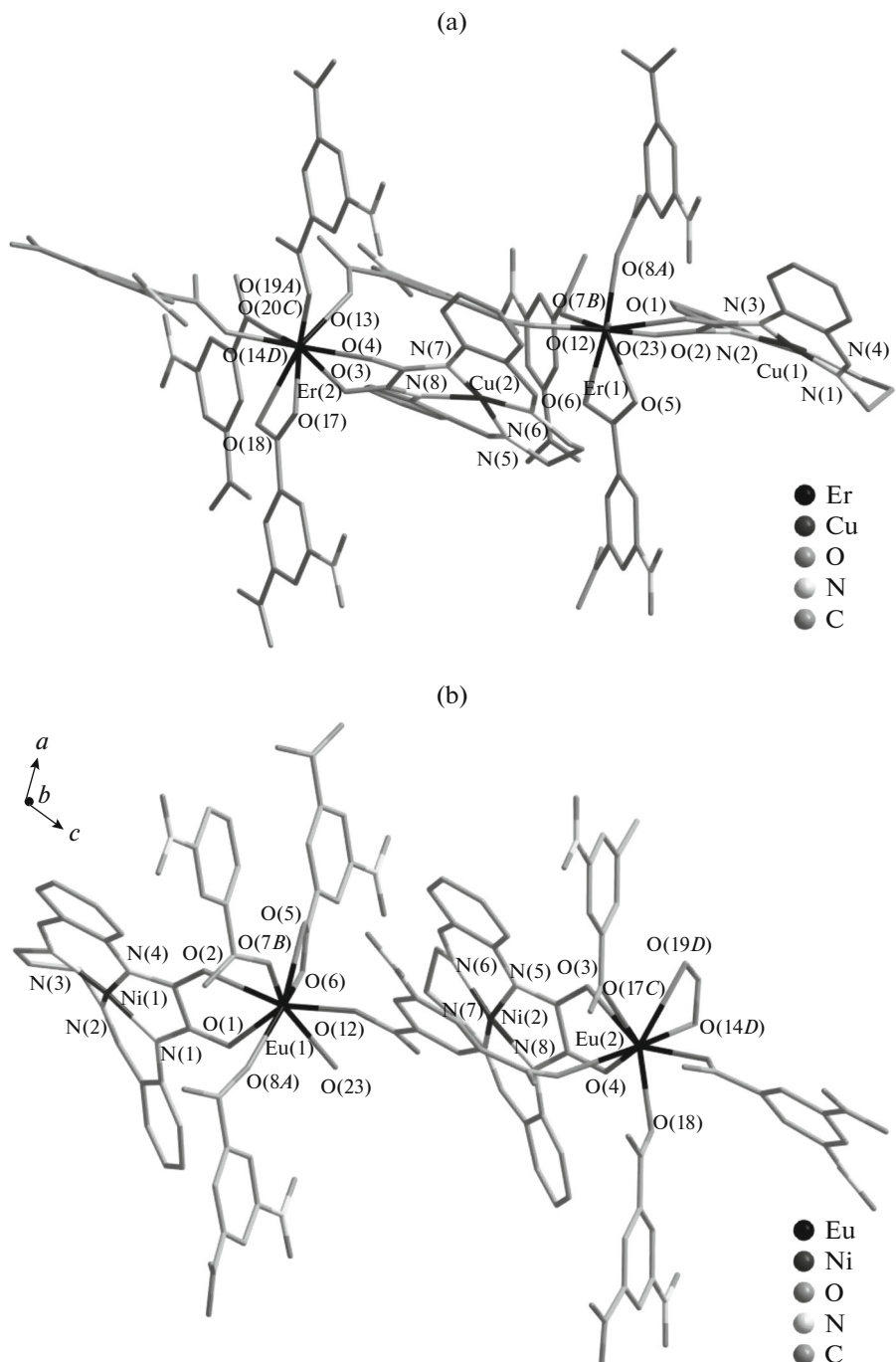


Fig. 1. Portion of the crystal structures of **I** (a) and **II** (b) showing coordinate environments of Er(III), Cu(II) and Eu(III), Ni(II) ions. All H atoms are omitted for clarity. Symmetry codes: (A) $1+x, y, z$; (B) $-x, -y, 2-z$; (C) $-1-x, -1-y, 1-z$; (D) $-x, -1-y, 1-z$ for **I** and (A) $-1-x, y, z$; (B) $2-x, -y, -z$; (C) $2-x, 1-y, 1-z$; (D) $1+x, y, z$ for **II**.

and Eu³⁺ ions were not observed, because the absorption intensity of them is very feebleness.

In order to study the effects of 5-nitroisophthalate and mononuclear macrocyclic oxamide complex CuL on the visible and near-infrared luminescence properties of Er³⁺ ions, the luminescence properties of the complex **I** using the excitation wavelength of 467 nm

was investigated in the solid state at room temperature. The main emission bands in the visible area are at 544, 591, and 615 nm, and these bands may be attributed to the $^2H_{11/2} \rightarrow ^4I_{15/2}$, $^4S_{3/2} \rightarrow ^4I_{15/2}$, and $^4F_{9/2} \rightarrow ^4I_{15/2}$ transitions of the Er³⁺ ion (Fig. 4). The NIR emission band of Er³⁺ ion at 1530 nm was also observed (Fig. 5), which can be assigned to the Er(III)-centered $f-f$

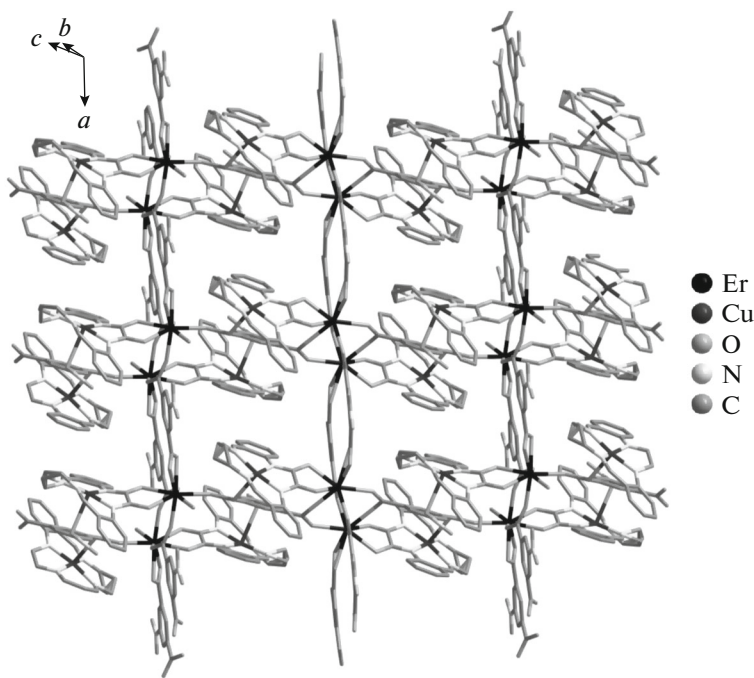


Fig. 2. The view of the self-assembly 2D framework bridged by Nip^{2-} and ML ligands for complex **I**.

transitions from the $^4I_{13/2}$ to the $^4I_{15/2}$ [22, 23, 26]. In order to further explore the cause of near infrared luminescence, the emission spectra of mononuclear macrocyclic oxamide complex CuL and 5-nitroisophthalic acid were also measured at $\lambda_{\text{ex}} = 467$ nm, the results show that the broad NIR phosphorescence of free CuL around 909 nm has been observed. Com-

pared with the NIR emission spectrum of CuL, the emission intensity of **I** around 909 nm distinctly decreases or disappears, which indicates that the efficient energy transfer from excited Cu(II) to the Er^{3+} excited state $^4I_{13/2}$ through the oxamide oxygen bridge has occurred, and eventually leads to the $f-f$ transition of Er(III) center in the NIR range [22, 23, 26]. Therefore, it can be concluded that the near infrared luminescence of Er(III) center is generated by CuL sensitization.

Thus, two new 3d–4f heterometallic coordination polymers Cu_2Er_2 and Eu_2Ni_2 were obtained with ML

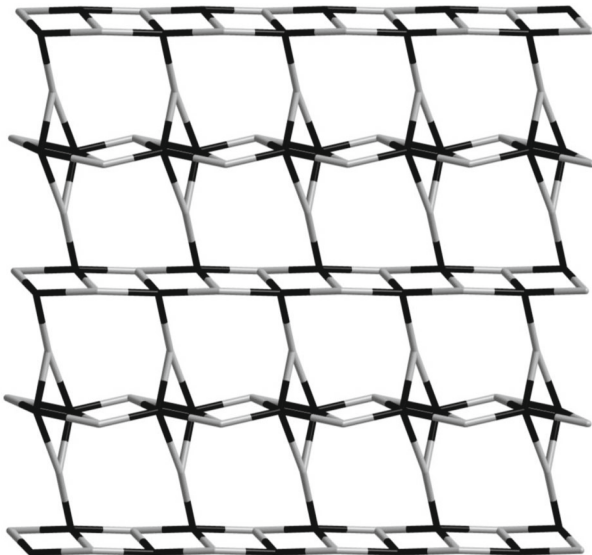


Fig. 3. The topological representation of the 2D sheet, the blue and pink sticks represent Nip^{2-} and Ln^{3+} ions ($\text{Ln} = \text{Er}$ (**I**), Eu (**II**)).

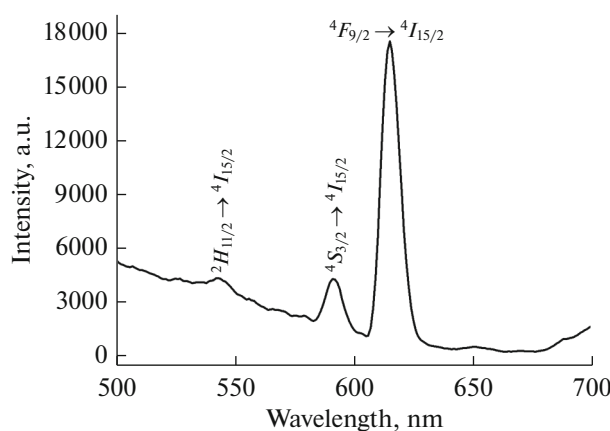


Fig. 4. Solid-state visible emission spectra of **I** ($\lambda_{\text{ex}} = 467$ nm).

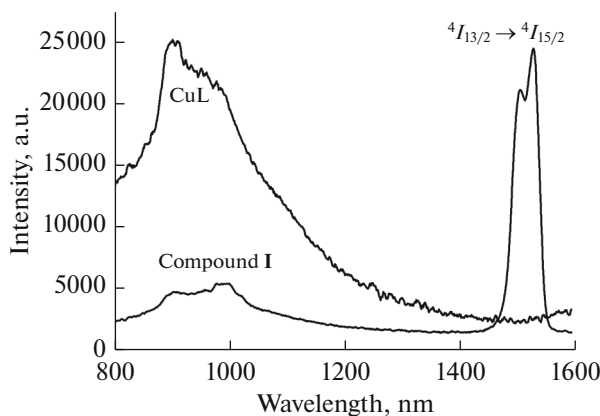


Fig. 5. Solid-state NIR emission spectra of **I** and CuL ($\lambda_{\text{ex}} = 467$ nm).

(M = Cu, Ni) and 5-nitroisophthalate as co-ligands under solvothermal reaction conditions. The single-crystal X-ray diffraction analyses indicate that compounds **I** and **II** are a 2D heterometallic framework with 3,3,4,5-connected (3.4.5)(3².4².5.6³.7²)(4².6³.8)(4².6) topology. The luminescence properties of complex **I** proved that mononuclear macrocyclic oxamide CuL can serve as an efficient sensitizer for the near-infrared luminescence of trivalent erbium ion.

FUNDING

This work was supported by Tianjin Normal University (no. 52XC1102). The program for innovative research team in University of Tianjin (TD12-5038) and the 111 project of Nankai University (111 project, B12015).

REFERENCES

1. Bazhina, E.S., Aleksandrov, G.G., Kiskin, M.A., et al., *Eur. J. Inorg. Chem.*, 2018, vol. 47, p. 5075.
2. Goldberg, A., Kiskin, M., Shalygina, O., et al., *Chem. Asian J.*, 2016, vol. 11, p. 604.
3. Kiskin, M., Zorina-Tikhonova, E., Kolotilov, S., et al., *Eur. J. Inorg. Chem.*, 2018, vol. 44, p. 1356.
4. Kiraev, S.R., Nikolaevskii, S.A., Kiskin, M.A., et al., *Inorg. Chim. Acta*, 2018, vol. 477, p. 15.
5. Sapianik, A.A., Zorina-Tikhonova, E.N., Kiskin, M.A., et al., *Inorg. Chem.*, 2017, vol. 56, p. 1599.
6. Zhang, J.W., Ren, Y.N., and Li, J.X., *Eur. J. Inorg. Chem.*, 2018, vol. 44, p. 1099.
7. Yang, M., Xie, J., Sun, Z., et al., *Inorg. Chem.*, 2017, vol. 56, p. 13482.
8. Zhou, G.J., Chen, W.P., Yu, Y.Z., et al., *Inorg. Chem.*, 2017, vol. 56, p. 12821.
9. Xie, W.P., Wang, N., Long, Y., et al., *Inorg. Chem. Commun.*, 2014, vol. 40, p. 151.
10. Wang, K., Chen, Z.L., Zou, H.H., et al., *Cryst. Growth Des.*, 2015, vol. 15, p. 2883.
11. Li, X.F., Huang, Y.B., Cao, R., et al., *Cryst. Growth Des.*, 2012, vol. 12, p. 3549.
12. Zhao, B., Cheng, P., Chen, X.Y., et al., *J. Am. Chem. Soc.*, 2004, vol. 126, p. 3012.
13. Yang, X.P., Lam, D., Chan, C., et al., *Dalton Trans.*, 2011, vol. 40, p. 9795.
14. He, X.X., Liu, Y., Lv, Y., et al., *Inorg. Chem.*, 2016, vol. 55, p. 2048.
15. Dong, R.T., Chen, X.L., Cui, X., et al., *CrystEngComm*, 2016, vol. 18, p. 5547.
16. Xin, N., Sun, Y.Q., Han, Y.N., et al., *Z. Anorg. Allg. Chem.*, 2016, vol. 642, p. 1460.
17. Sun, Y.G., Zong, W.H., Xiong, G., et al., *Polyhedron*, 2014, vol. 83, p. 68.
18. Xin, N., Sun, Y.Q., Zheng, Y.F., et al., *J. Solid State Chem.*, 2016, vol. 243, p. 267.
19. Bunck, D.N. and Dichtel, W.R., *Chem. Eur. J.*, 2013, vol. 19, p. 818.
20. Chen, S., Shuai, Q., and Gao, S.L., *Z. Anorg. Allg. Chem.*, 2008, vol. 634, p. 1591.
21. Ferrer, B., Alvaro, M., and Baldovi, H.G., *ChemPhysChem*, 2014, vol. 15, p. 924.
22. Chorazy, S., Arczynski, M., Nakabayashi, K., et al., *Inorg. Chem.*, 2015, vol. 54, p. 4724.
23. Dannenbauer, N., Matthes, P.R., Scheller, T.P., et al., *Inorg. Chem.*, 2016, vol. 55, p. 7396.
24. Guo, X.D., Zhu, G.S., Fang, Q.R., et al., *Inorg. Chem.*, 2005, vol. 44, p. 3850.
25. Boyer, J.C., Carling, C.J., Gates, B.D., et al., *J. Am. Chem. Soc.*, 2010, vol. 132, p. 15766.
26. Sorgho, L.A., Nozary, H., Aebischer, A., et al., *J. Am. Chem. Soc.*, 2012, vol. 134, p. 12675.
27. Chow, C.Y., Eliseeva, S.V., Trivedi, E.R., et al., *J. Am. Chem. Soc.*, 2016, vol. 138, p. 5100.
28. Hebbink, G.A., Le' on, L.G., Reinhoudt, D.N., et al., *J. Phys. Chem. A*, 2003, vol. 107, p. 2483.
29. Black, D.C.S. and Corrie, H., *Inorg. Nucl. Chem. Lett.*, 1976, vol. 12, p. 657.
30. Nakamoto, K., *Infrared, Raman Spectra of Inorganic and Coordination Compounds*, New York: John Wiley, 1997.
31. Lampeka, Y.D. and Gavriš, S.P., *Polyhedron*, 2000, vol. 19, p. 2533.